TREE-RING RESEARCH, *Vol. 74(1), 2018, pp. 28–38*
DOI: http://dx.doi.org/10.3959/1536-1098-74.1.28

ENSEMBLE EMPIRICAL MODE DECOMPOSITION AS AN ALTERNATIVE FOR TREE-RING CHRONOLOGY DEVELOPMENT

BIING T. GUAN[1]*, WILLIAM E. WRIGHT[1,2], and EDWARD R. COOK[3]

[1]School of Forestry and Resource Conservation, National Taiwan University, Taipei, 10617, Taiwan, Republic of China

[2]Laboratory of Tree-Ring Research, University of Arizona, Tucson, AZ, 85721, USA

[3]Tree-Ring Laboratory, Lamont-Doherty Earth Observatory, Columbia University, Palisades, NY, 10964, USA

ABSTRACT

Since its establishment, tree-ring analysis has benefitted several scientific fields. Because of its many advantages, dendrochronology is a first choice to reconstruct past environmental variability. Two major concerns about the current tree-ring reconstruction paradigm are the subjective choices of detrending functions and the lack of fidelity to data of chronology generation methods. It is difficult to recover the original tree-ring data once they have been detrended and standardized. In this study, ensemble empirical mode decomposition (EEMD) is introduced as an objective high-fidelity stand-alone approach for developing tree-ring chronologies. Basic concepts of EEMD, recommended steps in developing chronologies, and available public domain programs are discussed. To demonstrate the potentials of EEMD for chronology development, two examples are provided, one for climate and the other for streamflow reconstructions. In both examples, EEMD chronologies show higher correlations with the instrumental data and have more power in their spectra than the ones developed based on the current tree-ring reconstruction approach. General usage concerns and cautions are also addressed.

Keywords: empirical mode decomposition, ensemble empirical mode decomposition, intrinsic mode functions, nonlinear and non-stationary time series.

INTRODUCTION

In the years since A. E. Douglass published a series of seminal papers in the late 1910s and 1920s about the relationship between tree radial growth and climate, papers that laid the foundation for quantitative tree-ring analysis (dendrochronology), the discipline has benefitted many scientific fields (*e.g.* archaeology, climatology, ecology, hydrology) and enjoyed great successes, particularly in the last decade. In the 2015 edition of the Journal Citation Report, two major tree-ring analysis journals (*Tree-Ring Research* and *Dendrochronologia*) are listed among the top ten journals in the Forestry category. This evidence of the importance of dendrochronology may be ascribed mostly to recognition of the need to devise sound natural resource management plans and to assess the potential impacts of climate warming, a need best served through better understandings about past environment variability. The advantages of tree-ring analysis (*e.g.* precise dating, wide applicability, large number of replications, relatively low cost) have made the discipline a first choice for the task worldwide.

Tree-ring analysis comprises two basic stages, namely, field sampling-preparation and crossdating (Fritts 1976). For reconstructions, two additional stages are required, namely, chronology development and correlation-reconstruction. Procedures in the first two stages are well-established. For reconstructions, chronology development is the most critical procedure and determines the overall success, as an inappropriate chronology will lead to an inappropriate reconstruction.

Cook (1987) proposed that a ring width signal at any time t, R_t, comprises five additive components:

$$R_t = A_t + C_t + dD1_t + dD2_t + E_t, \qquad (1)$$

where A_t is the age-size related internal growth trend signal, C_t is the climate signal, $D1_t$ and $D2_t$

*Corresponding author: btguan@ntu.edu.tw

are endogenous and exogenous disturbance, respectively, and E_t is unexplainable random noise unrelated to the other signals. The binary variable δ indicates the absence (0) or presence (1) of the two types of disturbances in time t. This decomposition model is not only applicable to ring width, but other ring characteristics as well (*e.g.* maximum latewood density). Mainly because of the presence of trends in growth and in external parameters (*e.g.* warming), and perhaps low-frequency fluctuations in growth caused by variability in climate or by stand dynamics, tree-ring series are typically non-stationary (Cook *et al.* 1990). To conform to the classical time series analysis stationarity assumption (at least weak stationarity), the first step in developing a chronology is to detrend and standardize (Fritts 1976; Cook *et al.* 1990).

Next to crossdating, finding a suitable detrending function is likely the most important and challenging task of the entire tree-ring reconstruction. Among the detrending functions available in the *de facto* chronology development program ARSTAN (Cook and Holmes 1986), negative exponential function, cubic smoothing spline (Cook and Peters 1981), its generalization Hugershoff curve, and regional curve standardization (Briffa *et al.* 1992) are frequently used. As different functions may lead to drastically different chronologies (*e.g.* Sullivan *et al.* 2016), experience is required to achieve "optimal" detrending, conditional on the purpose of the tree-ring analysis being conducted.

However, from a statistical perspective, there are some serious issues involved in this step. First, applying a pre-selected detrending function amounts to injecting external (structural) information into data. Second, detrending may remove not only growth trend, but some low-frequency climate signals as well (Cook *et al.* 1995; Markonis and Koutsoyiannis 2016). Although methods like regional curve standardization (Briffa *et al.* 1992; Esper *et al.* 2002; Helama *et al.* 2016) and "signal-free" approach (Melvin and Briffa 2008) were developed to alleviate this problem, those methods are still preselected. Finally, one major concern about the current tree-ring reconstruction paradigm is its fidelity to data, where a high fidelity tree-ring chronology production method refers to one that can separate the common signal from individual tree-ring series variation and can recover the original tree-ring data from a chronology with simple arithmetic operations.

A recent advance in signal processing methods is ensemble empirical mode decomposition (EEMD), a highly efficient and adaptive method for processing non-linear and non-stationary signals (Wu and Huang 2009). This empirical method has been widely applied in many fields (*e.g.* engineering, Lei *et al.* (2009); geology, Wang *et al.* (2012); neuroscience, Guerrero-Mosquera *et al.* (2016)), including tree growth response to natural climate variability (Guan *et al.* 2012; Lo *et al.* 2017), trends in initial flowering phenology (Guan 2014), and tree-ring reconstruction of long-term climate variability (Shi *et al.* 2012; Zhang and Chen 2017).

In this study, we propose the use of EEMD as an alternative to develop tree-ring chronologies. However, unlike in the previous tree-ring applications, where EEMD was either used on already developed chronologies (Shi *et al.* 2012) or only as a method to detrend the individual ring series followed by traditional methods for indexing and chronology production (Zhang and Chen 2017), this study will show that EEMD can be used as a stand-alone alternative for chronology development.

BASIC CONCEPTS

Empirical Mode Decomposition

Huang *et al.* (1998) developed a method called empirical mode decomposition (EMD) to identify instantaneous frequencies embedded in a nonlinear and non-stationary series. EMD considers that, at any time t, a complex signal series $x(t)$ can be considered a superimposition of a small number of simple oscillatory functions (the intrinsic mode functions, IMFs) with significantly different frequencies and a residual term. In addition to the completeness (*i.e.* decomposable into a finite number of components while preserving all information) and the orthogonality that are required for a set of basis functions to represent a linear system, the IMFs are also required to be local and adaptive in order to span a nonlinear and non-stationary time series. Locality means that both the amplitude and the frequency, which change with time in a non-stationary series, need to be identified at the instance that they occur (*i.e.* as a function of time).

Adaptivity means that, to fully account for the underlying processes, the decomposition has to adapt to data-local variations. In a nonlinear series, it is impossible for an *a priori* selected function to fit the entire series; the basis functions (IMFs) representing a nonlinear system need to be derived from the data exclusively, hence the empirical nature of this method. EMD was developed to extract IMFs that have these four properties: completeness, orthogonality, locality, and adaptivity.

The extraction is a spline-based iterative sifting process. Let $x(t)$ be a time series, and the objective of EMD is to decompose $x(t)$ into a small and finite number of IMFs and a residual (trend):

$$x(t) = \sum_{i=1}^{k} IMF_i(t) + R(t), \qquad (2)$$

where k is the number of IMFs, $IMF_i(t)$ is the i^{th} IMF, and $R(t)$ is the residual. To avoid over-extraction, the number of IMFs is a function of data length, $k = \log_2(\text{length})-1$, rounded toward zero. A proper IMF needs to satisfy the following conditions: (1) the numbers of extrema and zero crossings must be equal or differ at most by one, and (2) the envelopes defined by the local maxima and minima must average to zero (Huang *et al.* 1998; Huang and Wu 2008).

The IMFs are extracted from high to low frequencies. EMD first finds the local extrema in $x(t)$ and generates a pair of upper and lower envelopes by interpolating local maxima and local minima using a cubic spline. It then takes the average of the two envelopes and subtracts the average from the original signal $x(t)$, producing an oscillatory series $x'(t)$. Treating $x'(t)$ as the new signal and by repeating the sifting (local envelopes finding-averaging-subtracting) steps, $x'(t)$ is further processed until it meets the conditions of an IMF.

Once an IMF is extracted, EMD subtracts it from $x(t)$ and sifts through the remaining part of $x(t)$ to extract the next IMF of lower frequency. The sifting process runs iteratively until the remaining signal is either constant, monotonic, or contains only one extremum over the data span considered, the $R(t)$ part of the decomposition. If the $R(t)$ is not constant, then it constitutes a trend (Huang *et al.* 1998; Huang and Wu 2008). Thus, from a tree-ring analysis perspective, EMD detrends a tree-ring series *a posteriori*. A detailed account on the EMD algorithm can be found in Huang and Wu (2008) and Kim and Oh (2009).

Under certain circumstances, EMD is essentially an efficient dyadic filter bank, that is, the mean period of an IMF is almost twice that of the previous one. IMFs can therefore be considered as band-pass filtered (Flandrin *et al.* 2004; Wu and Huang 2004).

Ensemble Empirical Mode Decomposition

A problem of EMD IMFs is mode mixing (a consequence of signal intermittency), that is, a frequency mode may reside in more than one IMF, and an IMF may contain more than one mode (Huang and Wu 2008). EEMD was developed to alleviate the problem. It is a Monte Carlo approach in which zero-mean Gaussian white noise is added to each EMD process to achieve better signal separation. An EEMD IMF or trend is simply the ensemble mean of the corresponding EMD IMFs or trends (Huang and Wu 2008; Wu and Huang 2009). Although some of the EEMD IMFs might not be true IMFs and might not be orthogonal to the others (Wu and Huang 2009), they are still suitable for developing tree-ring chronologies.

Because EMD/EEMD decomposes time-series based on local behaviors and in a sequential manner, there is no need to assume either the linearity or stationarity of the data. It also does not assume an *a priori* structure about the trend; it is derived intrinsically and adaptively (Wu *et al.* 2007). Finally, the approach preserves all signals, summing the IMFs and residual will recover the original data, which preserves the original unit of measure and allows us to evaluate the physiological relationship between a ring characteristic and the abiotic factor of interest in a meaningful way. These properties make EEMD a valuable new tool for development of tree-ring chronologies.

STEPS IN DEVELOPING CHRONOLOGIES

For reconstruction purpose, we recommend the following steps to develop chronologies:

Let RS_i be the i^{th} ring series $i = 1, 2, ..., m$, where m is the total number of ring series, and n be the maximum number of years among RS_i, *i.e.*, chronology length.

Step 1. FOR $i = 1$ to m:

Applying EEMD to detrend individual ring series RS_i, $Dt_i = RS_i - Tr_i$, where Dt_i is the detrended part and Tr_i is the EEMD extracted trend of RS_i

END

This step is much like the traditional approach and can be done in a batch mode using the same white noise distribution, typically a zero-mean Gaussian distribution, noise-level (*e.g.* 10% relative to the standard deviation of the input series), and ensemble size (*e.g.* 1000); or in an interactive mode with different noise-levels and ensemble sizes for different ring series.

Step 2. FOR $j = 1$ to n

$CC_j = Average\ (\sum_{i=1}^{m} Dt_i)$, where CC_j is the value of the combined chronology at year j

END

This step combines all the detrended parts chronologically and then averages them to obtain a combined chronology. One can use simple averaging, Tukey's bi-weight, or trimmed mean for the task.

Step 3. Applying EEMD to the combined chronology.

Step 4. Inspecting each IMF from the combined chronology, and determining the correlations between the IMFs. One may want to merge highly correlated IMFs.

Step 5. Exploring the relationships between IMFs and the instrumental data, starting from higher frequency IMFs, and incorporating IMFs of lower frequency sequentially until satisfied. Similar to developing a polynomial regression model, we recommend that if a lower frequency IMF is in a chronology, the higher frequency IMFs should also be retained as they represent fundamental variations. One may also want to use a stepwise regression model-building approach with the IMFs as the predictors to find the best model based on some criteria (*e.g.* the Akaike's information criterion, adjusted r^2).

COMPUTER PROGRAMS

There are probably many programs that can perform EMD/EEMD analyses. We will introduce only those that we are aware of, which are available in the public domain, and that can be executed in MATLAB or R environments.

MATLAB:

1. The Research Center for Adaptive Data Analysis, National Central University, Taiwan, R.O.C., with the inventor of EMD/EEMD Dr. Norden E. Huang as the director, maintains a MATLAB program which can be downloaded at http://rcada.ncu.edu.tw/research1.htm (Wu and Huang 2009). A fast EMD/EEMD code is also available. Besides programs, the website also has abundant resources to learn about the approach.
2. The Laboratorio de Señales y Dinámicas no Lineales Facultad de Ingeniería, Universidad Nacional de Entre Ríos, directed by Dr. María Eugenia Torres, maintains a program that can perform both EEMD and Complete EEMD (CEEMD) with Adaptive Noise (CCEMDAN) that can be downloaded at http://bioingenieria.edu.ar/grupos/ldnlys/metorres/re_inter.htm. The website also has an improved version of CEEMDAN (Colominas *et al.* 2014).

R:

1. EMD package: This is perhaps the first EMD package in R and has good documentation and conceptual diagram about the EMD algorithm (Kim and Oh 2009).
2. hht package: built upon EMD package, this package can perform CEEMD, EEMD, and many more (Bowman and Lee 2013).
3. Rlibeemd package: Ported from C codes, this package can perform CEEMDAN and EEMD, has fast execution speed for moderately large ensemble size, and is fully integrated with R's time series analysis functions and graphic environment (Luukko *et al.* 2016).

EXAMPLES

We present two reconstructions with chronologies completely developed using EEMD.

Example 1

The data are from the study of Wright *et al.* (2015). The species is Taiwan yellow false cypress (*Chamaecyparis obtusa* Sieb. & Zucc. var. *formosana* (Hayata) Rehder) from the northeastern mountain area of Taiwan. The data set had 50 cores

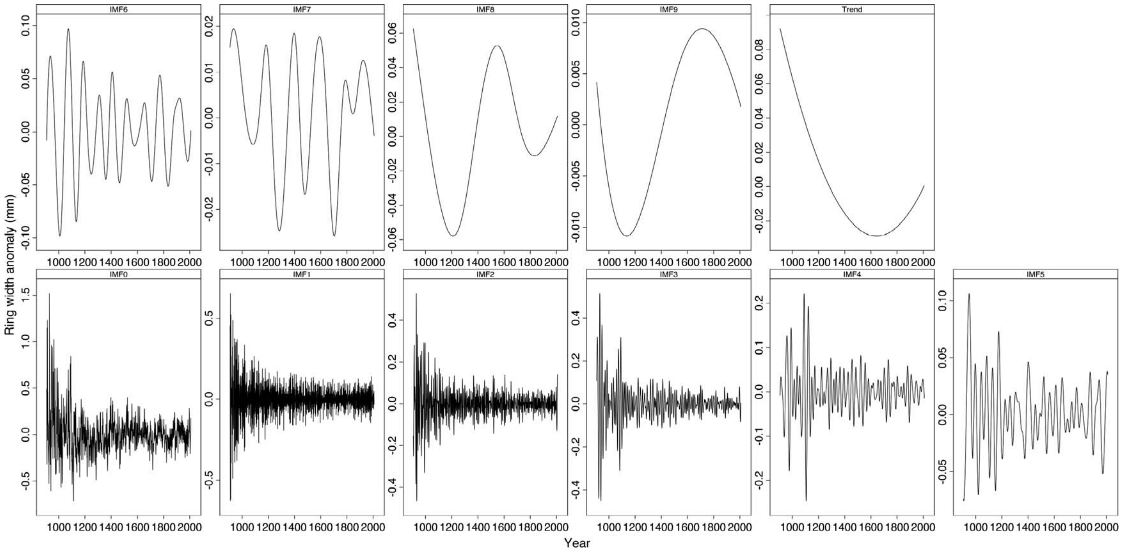

Figure 1. EEMD decomposition results of the combined ring width chronology of Taiwan yellow false cypress. IMF0 represents the combined chronology.

from 30 trees, covering the period from C.E. 907 to 2008.

Wright *et al.* (2015), using traditional methods of chronology production, found that a 5-yr 1^{st}-order loess high-pass filtered standard ring width chronology is significantly correlated with the 5-yr 1^{st}-order loess high-pass filtered average spring (March to May, MAM) Western Pacific pattern index (WPI; $r = -0.63$, $p < 0.001$, 95% confidence interval, CI, [−0.77, −0.42]) and East Asian Subtropical Jet Stream index (EAJI; $r = -0.56$, $p < 0.001$, 95% CI [−0.73, −0.33]) values from the previous year, between 1958 and 2006. Because the two indices are very closely related, the Western Pacific pattern can be considered as an indicator of Asian Subtropical Jet Stream intensity (Barnston and Livezey 1987). We demonstrate only the relationship with WPI here.

For the EEMD reanalysis, the 50 cores were first detrended using Rlibeemd with noise-levels being 10% of the standard deviation of each core and an ensemble size of 5000. Detrended components were then combined and averaged chronologically using simple averaging to obtain the combined chronology. EEMD was applied to the chronology using the same relative noise-level and ensemble size. Nine IMFs and a trend term resulted from the decomposition (Figure 1).

Among the IMFs, IMF1 was significantly correlated with the 5-year 1^{st}-order loess high-pass filtered average previous MAM WPI values ($r = -0.708$, $p < 0.001$, 95% CI [−0.825, −0.533]) in the 1958-2006 period. A slightly higher correlation was found between IMF1 and the filtered average previous February to May WPI values ($r = -0.714$, $p < 0.001$, 95% CI [−0.829, −0.541]). Split-period calibration-verification (1958-1982, 1983-2006) indicated that the regression functions based on the average previous MAM WPI and IMF1 had a significant autocorrelation at lag 1 (the Durbin-Watson test, $p < 0.05$) in the first period, and a significant autocorrelation at lag 2 ($p < 0.01$) in the second period. Similar situations also occurred in Wright *et al.* (2015), which used a generalized least square approach to remediate the problem. The regression functions based on the new relationship had no significant autocorrelation up to lag 5 in both periods (all $p > 0.05$). Both regression functions also met the normality (the Shapiro-Wilk test, all $p > 0.1$) and constant variance (the Breusch-Pagan test, all $p > 0.6$) assumptions.

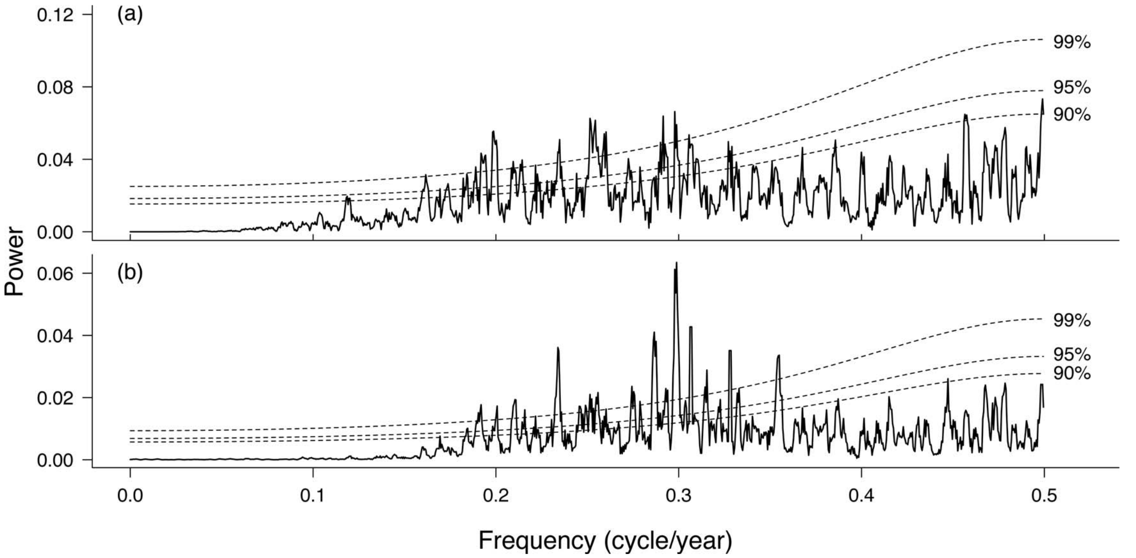

Figure 2. The multi-taper spectrum of Taiwan yellow false cypress ring width (a) EEMD IMF1 chronology and (b) 5-year 1st-order loess high-pass filtered standard chronology against a red-noise null hypothesis. The confidence levels are derived from the AR(1) process of each chronology.

The multi-taper spectra of the two chronologies showed that IMF1 had more power overall and more significant peaks ($p < 0.1$) at periodicity greater than 5 years (Figure 2). Statistics used to assess the performance of the split-period calibration-verification based on the new relationship, including the coefficient of determination (r^2), reduction of error (RE), and coefficient of efficiency (CE) are given in Table 1. Compared to those in Wright *et al.* (2015), the new relationship was more stable temporally and also included the late winter month. Thus, IMF1 should be able to provide a good millennial-length reconstruction of late winter to spring high frequency variability of WPI and EAJI.

Table 1. The split-period calibration-verification statistics of Example 1 with IMF1 as the independent variable and the 5-year 1st-order loess high-pass filtered average previous February to May Western Pacific pattern index values as the dependent variable.

Calibration		Verification		
Period	r^{2*}	Period	RE*	CE*
1958–1982	0.51	1983–2006	0.51	0.51
1983–2006	0.52	1958–1982	0.50	0.50

*r^2 = Coefficient of determination, RE = Reduction of error, CE = Coefficient of efficiency.

Example 2

The data are from a local stream flow reconstruction study. The objective of the study was to reconstruct the dry season (October to March) stream flow regime of the Chichiawan Stream of central Taiwan, the sole existing natural habitat of Formosa landlocked salmon (*Oncorhynchus formosanus* Jordan & Oshima), an IUCN-listed critically endangered species. The tree species is Taiwan Douglas-fir (*Pseudotsuga wilsoniana* Hayata; TDF), and 41 living TDF were sampled near the stream (24°21′N, 121°19′E, elevations 1700 to 1900 m). Streamflow data were from an automatic gauging station of the Taiwan Power Company (ID: 02505, 24°19′56″N, 121°17′38″E, elevation 1629 m). Because the dry season coincides with the dormant season of TDF, only earlywood (EW) ring widths were suitable for the reconstruction. A total of 57 cores were selected for the reconstruction, covering the period from 1642 to 2009. Instead of reconstructing streamflow directly, to place the flow regime in a probabilistic, event-based perspective and to stabilize flow data variance, the target of the reconstruction was standardized streamflow index (SSFI) based on the concept of standardized precipitation index (McKee *et al.* 1993; Vicente-Ser-

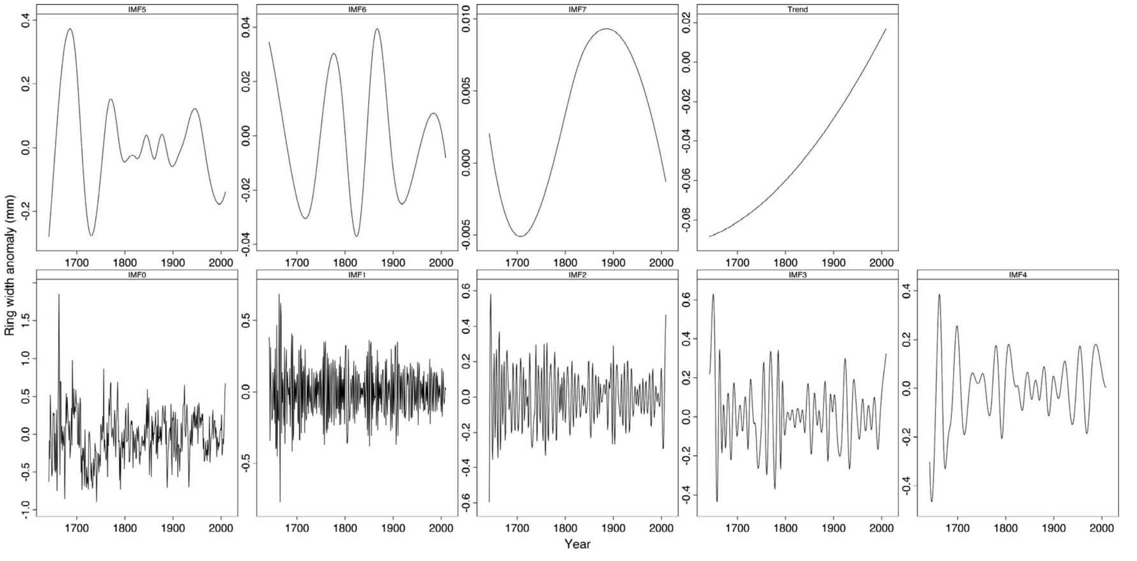

Figure 3. EEMD decomposition results of the earlywood ring width combined chronology of Taiwan Douglas fir. IMF0 represents the combined chronology.

rano *et al.* 2012). From October 1967 to March 2008, a series of SSFI were derived with resolutions from one to six months.

Two approaches were used to develop chronologies. Using ARSTAN, a smoothing spline with a window size of 50 years was used to detrend individual cores, and three chronologies (*i.e.* standard, residual, and ARS) were developed. EEMD with the same procedure and parameter settings as Example 1 was used to extract IMFs and trend, which resulted in seven IMFs and a trend (Figure 3).

Among the ARSTAN chronologies, the highest correlation was found between the 15-yr 1st-

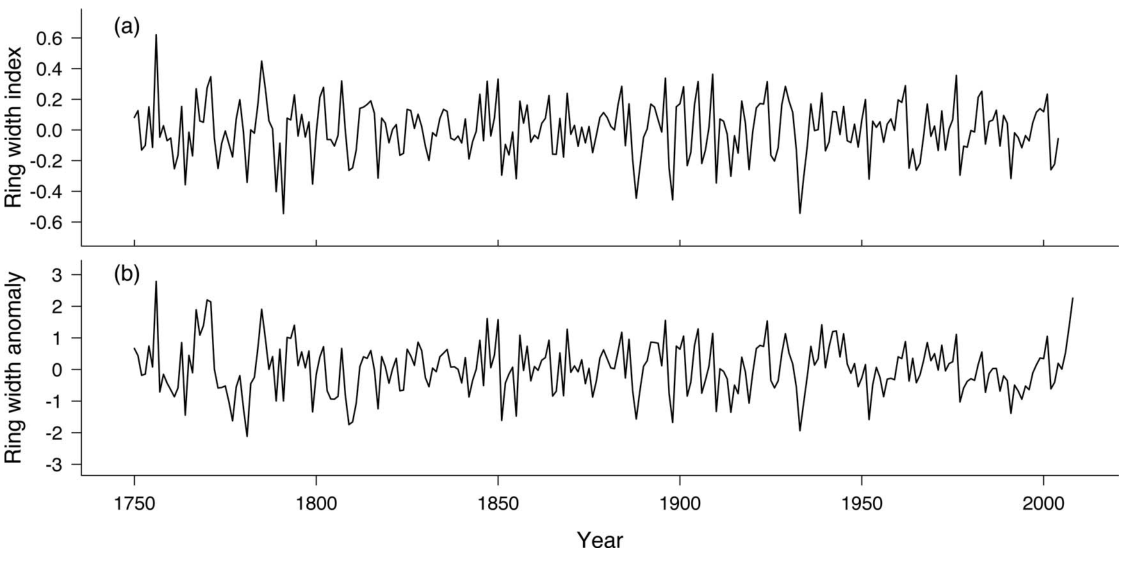

Figure 4. Taiwan Douglas-fir earlywood ring width (a) 15-year 1st-order loess high-pass filtered ARS chronology and (b) IMF1234 chronology since 1750.

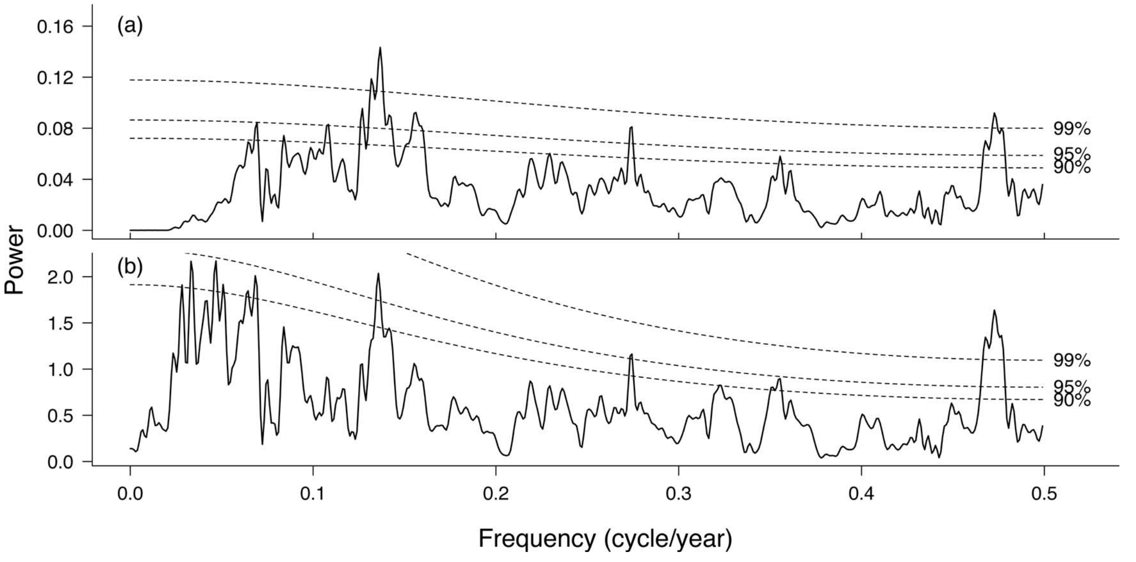

Figure 5. The multi-taper spectrum of Taiwan Douglas-fir earlywood ring width (a) 15-year 1st-order loess high pass filtered ARS chronology and (b) IMF1234 chronology against a red-noise null hypothesis. The confidence levels are derived from the AR(1) process of each chronology.

order loess high-pass filtered ARS chronology (ARS HP15, Figure 4*a*) and November to March SSFI in the 1968–2004 period ($r = 0.64$, $p < 0.001$, 95% CI [0.38, 0.79]; four years were lost because of filtering).

Stepwise model selection based on the Akaike's information and adjusted r^2 criteria identified that the model with the sum of first three IMFs, IMF123, and IMF4 as predictors and October to February SSFI ($SSFI_{OF}$) as the response variable was the best model. Based on the fitted values of that model, we constructed a new chronology, IMF1234 (Figure 4*b*), which explained about 50% of the variability in $SSFI_{OF}$. The correlations between IMF123 and IMF4 in the 1750–2008 and 1968–2008 periods were all not significant (all $p > 0.5$). The correlation between IMF123 alone and $SSFI_{OF}$ was about 0.65 ($p < 0.001$, 95% CI [0.43, 0.80]).

The multi-taper spectra of ARS HP15 and IMF1234 showed that the shapes of the two spectra were similar in the higher frequency part (periodicity less than 4 years; Figure 5), but IMF1234 had more significant peaks ($p < 0.1$) in the lower frequency region.

Although the split-period calibration-verification statistics of the two chronologies indicated that both chronologies were temporally stable and suitable for reconstruction (Tables 2 and 3), IMF1234 should provide a better reconstruction

Table 2. The split-period calibration-verification statistics of Example 2 with IMF1234 as the independent variable and the derived October to February standardized stream flow index as the dependent variable.

Calibration		Verification		
Period	r^{2*}	Period	RE*	CE*
1968–1989	0.46	1990–2008	0.47	0.46
1990–2008	0.57	1968–1989	0.42	0.41

*r^2 = Coefficient of determination, RE = Reduction of error, CE = Coefficient of efficiency.

Table 3. The split-period calibration-verification statistics of Example 2 with ARS HP15 as the independent variable and the derived November to March standardized stream flow index as the dependent variable.

Calibration		Verification		
Period	r^{2*}	Period	RE*	CE*
1968-1986	0.39	1987-2004	0.45	0.44
1987-2004	0.44	1968-1986	0.40	0.39

*r^2 = Coefficient of determination, RE = Reduction of error, CE = Coefficient of efficiency.

because of the presence of some lower frequency signals and a higher r^2 value.

DISCUSSION

In the two examples, the chronologies developed by using EEMD showed higher correlations with the instrumental data and had more power in their spectra than those developed based on the current tree-ring reconstruction approach (Tables 1–3; Figures 2 and 5). In the first example, the calibration function based on EEMD chronology also showed no autocorrelation in its residuals. Our examples demonstrate that tree-ring chronologies can be developed relatively easily using EEMD alone. Furthermore, all information contained in the original tree-ring measurement series is preserved.

Only the higher frequency IMFs were used to develop chronologies in the examples. In the first example, this was because the chronology and WPI in Wright *et al.* (2015) were high-pass filtered, so only IMF1 was needed for comparison purposes. In the second example, this was because of the length of the instrumental data, which was about 40 years, and the method used to select the predictors. Chronologies built in this manner contain only low-frequency variations that are supported by the instrumental data. However, whether this property is a limitation for reconstructions is still an open question. A recent study by Markonis and Koutsoyiannis (2016) suggested that some of the tree-ring based climate reconstructions could have more extreme events than there actually were. With longer instrumental data, we believe IMFs of lower frequency will be incorporated into a chronology.

Of the two parameters controlling the outcomes of EEMD, our experiences suggest that the introduced noise-level has a greater impact, particularly in detrending individual cores. It would require some fine tuning to find an appropriate noise-level. A level of 10% of the standard deviation of the input series is a good initial start (Wu and Huang 2009). A larger ensemble size will tend to eliminate the influences of the introduced noise. Depending on one's tolerance of numerical errors and time constraint, an ensemble size of a few hundreds to a few thousands will be adequate (Wu and Huang 2009; Guan 2014). Because EEMD is a Monte Carlo approach, it can be executed in parallel, which can be achieved easily in today's multi-core computing environments. In addition, as available EEMD programs are all developed for mathematical-statistical computing environments, such as MATLAB or R, we can do initial data processing, conduct exploratory data analysis, develop chronologies, visualize the results, and perform subsequent analyses in a fully integrated manner. However, this is not to say that we can simply let EEMD do the chronology development. As Example 2 demonstrated, to develop good chronologies, thorough data exploration to understand the relationships between IMFs and the response variables is still required.

CONCLUSIONS

In this study, we introduce EEMD as a valuable alternative for developing tree-ring chronologies. Removal of *a priori* (*e.g.* subjective) choices during detrending the individual tree-ring time series is the principle benefit of EEMD chronology production, although additional benefits related to retention of climate-related low-frequency signals are also expected in many applications. We briefly discuss the basic concepts of the approach, suggesting steps in developing chronologies, and available programs. General usage concerns and cautions are also addressed. We also offer two examples that demonstrate the potentials of using EEMD as a stand-alone approach for tree-ring chronology development, and in both cases EEMD chronologies perform better than the ones developed based on the current tree-ring reconstruction approach. It is our belief that EEMD will be a valuable addition to the existing methods for developing tree-ring chronologies.

ACKNOWLEDGMENTS

BTG was partially funded by the Ministry of Science and Technology, Taiwan, ROC (MOST 101-2313-B-002-015-MY3, MOST 102-2628-B-002-013-MY3) and by National Taiwan University. LDEO contribution number 8173.

REFERENCES CITED

Barnston, A. G., and R. E. Livezey, 1987. Classification, seasonality and persistence of low-frequency atmospheric circulation patterns. *Monthly Weather Review* 115:1083–1126. doi:10.1175/1520-0493(1987)115<1083:Csapol>2.0.Co;2.

Bowman, D., and J. Lees, 2013. The Hilbert-Huang Transform: A high resolution spectral method for nonlinear and nonstationary time series. *Seismological Research Letters* 84:1074–1080. doi: 10.1785/0220130025.

Briffa, K. R., P. D. Jones, T. S. Bartholin, D. Eckstein, F. H. Schweingruber, W. Karlen, P. Zetterberg, and M. Eronen, 1992. Fennoscandian summers from AD 500: Temperature-changes on short and long timescales. *Climate Dynamics* 7:111–119. doi:10.1007/BF00211153.

Colominas, M. A., G. Schlotthauer, and M. E. Torres, 2014. Improved complete ensemble EMD: A suitable tool for biomedical signal processing. *Biomedical Signal Processing and Control* 14:19–29. doi:10.1016/j.bspc.2014.06.009.

Cook, E. R., 1987. The decomposition of tree-ring series for environmental studies. *Tree-Ring Bulletin* 47: 37–59.

Cook, E. R., K. Briffa, S. Shiyatov, V. Mazepa, and P. D. Jones, 1990. Data analysis. In *Methods of Dendrochronology: Applications in the Environmental Science*, edited by Cook, E. R., and L. A. Kairiukstis, pp. 97–162. Kluwer, Dordercht, the Netherlands.

Cook, E. R., and R. L. Holmes, 1986. Users manual for program ARSTAN. Laboratory of Tree-Ring Research, University of Arizona, Tucson, USA.

Cook, E. R., and K. Peters, 1981. The smoothing spline: a new approach to standardizing forest interior tree-ring width series for dendroclimatic studies. *Tree-Ring Bulletin* 41: 45–53.

Cook, E. R., K. R. Briffa, D. M. Meko, D. A. Graybill, and G. Funkhouser, 1995. The segment length curse in long tree-ring chronology development for paleoclimatic studies. *The Holocene* 5:229–237. doi:10.1177/095968369500500211.

Esper, J., E. R. Cook, and F. H. Schweingruber, 2002. Low-frequency signals in long tree-ring chronologies for reconstructing past temperature variability. *Science* 295:2250–2253. doi:10.1126/science.1066208.

Flandrin, P., G. Rilling, and P. Goncalves, 2004. Empirical mode decomposition as a filter bank. *IEEE Signal Processing Letters* 11:112–114. doi:10.1109/Lsp.2003.821662.

Fritts, H. C., 1976. *Tree Rings and Climate*. Academic Press, London, UK.

Guan, B. T., 2014. Ensemble empirical mode decomposition for analyzing phenological responses to warming. *Agricultural and Forest Meteorology* 194:1–7. doi:10.1016/j.agrformet.2014.03.010.

Guan, B. T., W. E. Wright, C. H. Chung, and S. T. Chang, 2012. ENSO and PDO strongly influence Taiwan spruce height growth. *Forest Ecology and Management* 267:50–57. doi:10.1016/j.foreco.2011.11.028.

Guerrero-Mosquera, C., G. Borragán, and P. Peigneux, 2016. Automatic detection of noisy channels in fNIRS signal based on correlation analysis. *Journal of Neuroscience Methods* 271:128–138. doi: 10.1016/j.jneumeth.2016.07.010.

Helama, S., T. M. Melvin, and K. R. Briffa, 2016. Regional curve standardization: State of the art. *The Holocene* doi:10.1177/0959683616652709.

Huang, N. E., Z. Shen, S. R. Long, M. L. C. Wu, H. H. Shih, Q. N. Zheng, N.-C. Yen, C. C. Tung, and H. H. Liu, 1998. The empirical mode decomposition and the Hilbert spectrum for nonlinear and non-stationary time series analysis. *Proceedings of the Royal Society A: Mathematical Physical and Engineering Sciences* 454:903–995. doi:10.1098/rspa.1998.0193.

Huang, N. E., and Z. H. Wu, 2008. A review on Hilbert-Huang transform: Method and its applications to geophysical studies. *Reviews of Geophysics* 46. doi:10.1029/2007rg000228.

Kim, D., and H. S. Oh, 2009. EMD: A package for empirical mode decomposition and Hilbert spectrum. *The R Journal* 1:40–46.

Lei, Y., Z. He, and Y. Zi, 2009. Application of the EEMD method to rotor fault diagnosis of rotating machinery. *Mechanical Systems and Signal Processing* 23:1327–1338. doi: 10.1016/j.ymssp.2008.11.005.

Lo, Y. H., J. A. Blanco, and B. T. Guan, 2016. Douglas-fir radial growth in interior British Columbia can be linked to long-term oscillations in Pacific and Atlantic sea surface temperatures. *Canadian Journal of Forest Research* 47:371–381. doi:10.1139/cjfr-2016-0203.

Luukko, P. J. J., J. Helske, and E. Räsänen, 2016. Introducing libeemd: A program package for performing the ensemble empirical mode decomposition. *Computational Statistics* 31:545–557. doi:10.1007/s00180-015-0603-9.

Markonis, Y., and D. Koutsoyiannis, 2016. Scale-dependence of persistence in precipitation records. *Nature Climate Change* 6:399–401. doi: 10.1038/nclimate2894.

McKee, T. B., N. J. Doesken, and J. Kleist, 1993. The relationship of drought frequency and duration to time scales. *Proceedings of the 8th Conference on Applied Climatology*, Vol. 17, No. 22. American Meteorological Society, Boston, MA.

Melvin, T. M., and K. R. Briffa, 2008. A "signal-free" approach to dendroclimatic standardisation. *Dendrochronologia* 26:71–86. doi:10.1016/j.dendro.2007.12.001.

Shi, F., B. Yang, L. von Gunten, C. Qin, and Z. Y. Wang, 2012. Ensemble empirical mode decomposition for tree-ring climate reconstructions. *Theoretical and Applied Climatology* 109:233–243. doi:10.1007/s00704-011-0576-8.

Sullivan, P. F., R. R. Pattison, A. H. Brownlee, S. M. Cahoon, and T. N. Hollingsworth, 2016. Effect of tree-ring detrending method on apparent growth trends of black and white spruce in interior Alaska. *Environmental Research Letters* 11, 114007. doi:10.1088/1748-9326/11/11/114007.

Vicente-Serrano, S. M., J. I. Lopez-Moreno, S. Begueria, J. Lorenzo-Lacruz, C. Azorin-Molina, and E. Moran-Tejeda, 2012. Accurate computation of a streamflow drought index. *Journal of Hydrologic Engineering* 17:318–332. doi:10.1061/(Asce)He.1943-5584.0000433.

Wang, T., M. Zhang, Q. Yu, and H. Zhang 2012. Comparing the applications of EMD and EEMD on time–frequency analysis of seismic signal. *Journal of Applied Geophysics* 83:29–34. doi:10.1016/j.jappgeo.2012.05.002.

Wright, W. E., B. T. Guan, Y. H. Tseng, E. R. Cook, K. Y. Wei, and S. T. Chang, 2015. Reconstruction of the springtime East Asian subtropical jet and Western Pacific pattern from a millennial-length Taiwanese tree-ring chronology. *Climate Dynamics* 44:1645–1659. doi:10.1007/s00382-014-2402-3.

Wu, Z. H., and N. E. Huang, 2004. A study of the characteristics of white noise using the empirical mode decomposition method. *Proceedings of the Royal Society A: Mathematical Physical and Engineering Sciences* 460:1597–1611. doi:10.1098/rspa.2003.1221.

Wu, Z. H., and N. E. Huang, 2009. Ensemble empirical mode decomposition: A noise-assisted data analysis method. *Advances in Adaptive Data Analysis* 1:1–41. doi:10.1142/S1793536909000047.

Wu, Z. H., N. E. Huang, S. R. Long, and C. K. Peng, 2007. On the trend, detrending, and variability of nonlinear and nonstationary time series. *Proceedings of the National Academy of Sciences of the United States of America* 104:14889–14894. doi:10.1073/pnas.0701020104.

Zhang, X. L., and Z. J. Chen, 2017. A new method to remove the tree growth trend based on ensemble empirical mode decomposition. *Trees* 31(2): 405–413. doi:10.1007/s00468-015-1295-z.

Received 13 January 2017; accepted 27 May 2017.